Published by IOP Publishing for Sissa Medialab

Received: *November 6, 2019*
Revised: *December 17, 2019*
Accepted: *January 10, 2020*
Published: *February 24, 2020*

# An octagonal star shaped flexible UWB antenna with band-notched characteristics for WLAN applications

**S. Lakrit,[a,1] S. Das,[b] B.T.P. Madhav[c] and K. Vasu Babu[d]**

[a] *Smart Communications Research Team (ERSC), EMI, Mohammed V University in Rabat, Avenue Ibn Sina B.P 765, Agdal Rabat 10090, Morocco*

[b] *Department of ECE, IMPS College of Engineering and Technology, Chandipur, West Bengal 732103, India*

[c] *Department of ECE, Koneru Lakshmaiah Education Foundation, Vaddeswaram, Andhra Pradesh 522502, India*

[d] *Department of ECE, Vasireddy Venkatadri Institute of Technology Guntur, Nambur, Andhra Pradesh 522508, India*

*E-mail:* lakritsoufian@gmail.com

Abstract: In this paper, a flexible UWB antenna with band notched characteristics for high speed WLAN applications is presented. The flexibility of the designed antenna is achieved by developing the antenna on a flexible Teflon substrate. The proposed antenna primarily consists of a slot loaded octagonal star-shaped patch with a partial ground plane for wide operating bandwidth. A split ring resonator (SRR) based stop band filter is embedded in the ground plane to realize a rejection band characteristic to mitigate the interference impact from wireless local area network (WLAN) IEEE802.11n (5.725–5.825 GHz) band. The measured result shows that the suggested antenna operates over 3.25 to 13 GHz with a fractional bandwidth of about 120% with a peak gain of 6.7 dBi. The measurement results also confirm the presence of the rejection band from 5.7–6.2 GHz. Also, in terms of flexibility, the antenna provides high robustness in the performance for different types of bending conditions. The obtained results depict that the proposed antenna is suitable for mounting on all types of surface area with band rejection characteristics.

Keywords: Antennas; Microwave Antennas

[1]Corresponding author.


https://doi.org/10.1088/1748-0221/15/02/P02021

2020 JINST 15 P02021

## Contents





## 1 Introduction

The research and development of flexible or bendable antennas are increasing rapidly in wireless communication due to their numerous advantages such as easy to mount, highly durable, stretchable, resistance to corrosion, etc. These advantages enable the flexible antenna to be used in several fields of application such as radio frequency identification (RFID) tags, smart conformal devices, vehicle communication, strain sensors, flexible displays and internet of things (IoT). The flexibility nature is easily achieved by printing the radiating elements on the flexible substrate. Consequently, the flexible antennas can be mounted on the virtually at any place even on a curved surface. Apparently, the antenna structures designed using flexible substrate can withstand in every practical situation (i.e. folding, stretching, and bending) without major deviation in radiation performance. Now a days, the ultra-wideband technology is a popular area of applications for the implementation of flexible antenna as it covers a wide range of frequencies (3.1 GHz–10.6 GHz) as stated by the FCC [1] and two bands MB-OFDM (3.1 GHz–4.8 GHz) and DS-UWB (6 GHz–8.5 GHz) as stated by CEPT's ECC [2]. Actually, the adaptability of a flexible antenna can be increased by supporting this ultra-wideband frequency spectrum as it covers almost all of the wireless application frequency bands within its designated bandwidth. The UWB antenna also has some additional features including high data rate within its operating frequency band at very low power consumption for short-range communication. These features encourage the researchers to design UWB antenna by several techniques such as cylindrical DRA (dielectric resonator antenna) and Vivaldi antenna [3, 4]. However, the electromagnetic interference of high speed WLAN (5.725–5.825 GHz) provides a great threat towards the ultra-wide band antenna. Thus, the band notch characteristics can be established in order to eliminate such kind of electromagnetic interference for UWB antenna. Over the last few years, researchers have developed and applied several types of band notch techniques on UWB antenna such as inserting slot on patch elements [5], open loop resonator [6], Split ring resonator (SRR) [7], using fork shaped resonator [8] etc. Researchers have also focused on the design of flexible UWB antennas. In ref. [9], an ultra-wideband antenna is developed on two different kinds of substrates for wireless body area network application. The flexible RT/Duroid 5880 and rigid FR4 both are used for the fabrication of the antenna with the dimension of 86 mm × 72 mm and 75 mm × 61 mm, respectively. Both antennas provide almost similar operating bandwidth but the antenna designed with flexible substrate offers a better gain performance of 4.89 dBi. In the herein cited study [10], an ultra-wideband antenna on a relatively larger (48 mm × 34.9 mm) flexible polymer-based substrate provides an impedance bandwidth of 7 GHz with the peak gain of about 3.1 dBi at 5.8 GHz. In ref. [11], a CPW feed monopole antenna using flexible LCP substrate is presented for ultra-wideband frequency (2.5–11 GHz) with 4.2 dBi of peak gain but without band rejection capability. Another flexible UWB antenna on a thin kapton substrate with the dimension of 127 mm × 25 mm is demonstrated in [12] that supports 4G LTE bands within its frequency range. In the herein cited study [13], an inverted F-shaped ultra-wideband antenna on a flexible polyimide substrate is presented that covers the frequency band from 3.09 GHz to 11.96 GHz. In ref. [14], another ultra-wideband antenna using a circular radiator on a flexible photo paper is presented that provides an average gain of 4.87 dBi with the radiation efficiency of about 86.61%. A polymer fabric based circular UWB antenna on a 40 mm × 50 mm substrate is developed that provides consistent performance in terms of gain and $S_{11}$ in both bending and normal conditions [15]. In the herein cited study [16], a CPW fed antenna is developed on a flexible composite transparent substrate for covering ultra-wideband frequency range that also provides UWB characteristics in bending condition. In ref. [17], a microstrip line fed circular radiator based antenna on a textile substrate is presented for providing ultra-wideband operating frequency from 3 GHz to 12 GHz. In the herein study [18], a UWB antenna is developed on a large 97 mm × 88 mm felt substrate that covers a wide range of frequency (3.4 to 10.3 GHz) within its operating range. Abbasi et al. [19] designed an ultra-wideband antenna on a very thin flexible liquid crystal polymer substrate that provides rejection band cantered at 5.25 GHz to alleviate interference impact of WLAN band (5.15–5.35 GHz).

In this article, a compact flexible ultra-wideband antenna with band rejection characteristics for WLAN applications is proposed. The flexibility performance along with the wide band notched function is explored using an octagon star-shaped monopole radiator. A slot loaded octagon shaped patch element with the defected ground structure on a thin substrate are responsible for −10 dB superior ultra-wide impedance bandwidth from 3.25 to 13 GHz with a peak gain of 6.7 dBi. In this proposed structure, a ring-shaped split ring resonator is printed on the ground plane that acts like a band reject filter for generating notched band. Here, the slot line width of the SRR is varied to achieve adjustable band-notch characteristics. The measured rejection band of the proposed antenna mitigates the interference from wireless local area network (WLAN) IEEE802.11n (5.725–5.825 GHz) band. The flexible characteristics of the antenna are analysed by several types of bending test. In the aspect of flexibility, it is noted that the antenna provides negligible deviation in its return loss performance during bending deformations. The advantages of the proposed flexible antenna are as follows:

i. **Antenna dimension:** the overall volume of the proposed antenna is $42.5 \times 30 \times 0.6\,\text{mm}^3$, which is very attractive for the applications and easy integration of the designed antenna in UWB communication systems.

ii. **Wide bandwidth:** the proposed antenna provides significant operating bandwidth (3.25 GHz to 13 GHz) to cover total bandwidth requirements of UWB systems and many other modern wireless communication systems.

iii. **High gain:** the proposed antenna ensures an attractive peak gain of about 6.7 dBi which is expected for the desired UWB systems.

iv. **Band rejection capability:** the proposed antenna confirms the presence of a 500 MHz notched band (5.7 GHz to 6.2 GHz) for eliminating the interference from high speed WLAN (5.725–5.825 GHz) with UWB systems by introducing one single loop SRR in comparison to the reference work [7] in which a non flexible UWB antenna was proposed with band rejection for WLAN by using four multi loop RSSR on the radiating patch.

v. **Flexibility:** the proposed antenna maintains its UWB characteristics with the existence of a notched band for WLAN in the flexible or folded conditions.

## 2 Design approach

### 2.1 Design of flexible UWB antenna

The design of the antenna is initialized by selecting a thin flexible material that can be easily mounted on any surface and also provides high robustness in real life conditions such as bending. For the design of the proposed antenna, a small piece of 0.6 mm thick Teflon sheet was selected as a substrate for lightweight and robustness. The relative permittivity of the substrate is 2.08 and loss tangent is 0.001. The basic structure of the antenna includes a slot loaded octagonal star-shaped patch excited by 50-ohm microstrip line and the partial ground plane. The stepwise design evolution of the proposed UWB antenna is shown in figure 1 and the corresponding reflection coefficients for each design steps are shown in figure 2. Initially, a slot-loaded octagonal star-shaped patch on the partial ground (Antenna-A) is designed as shown in figure 1a. This Antenna-A does not meet the requirements of UWB frequency (3.1–10.6 GHz) range. It supports only 6.0 to 8.1 GHz frequency band as shown in figure 2. The Antenna-B shows the first step of modification by inserting a slot on the partial ground plane just below the feed line as shown in figure 1b. The incorporated slot improves the impedance bandwidth of the proposed antenna. The bandwidth of the antenna gets wider by 4800 MHz and the new operating bandwidth of the antenna ranges from 3.8 to10.7 GHz [see figure 2 (Antenna-B)]. Finally, it is observed from figure 1c that the further modification of the ground slot has enhanced the operating bandwidth of the proposed antenna and the achieved ultra wideband ranges from 3.1 to 12.7 GHz. The optimized dimension of the proposed UWB antenna is listed in table 1. Figure 2 clearly depicts that the proposed antenna meets the bandwidth requirements of UWB systems.

### 2.2 Parametric study

Some essential parameters of the antenna are studied to depict their effect on the antenna performance. Figure 3 shows the influences of these parameters on the proposed UWB antenna. Figure 3a shows a significant variation of reflection coefficients with ground slot width “w”. The antenna provides dual wideband (2.75–3.1 GHz), and (5.56–10 GHz) characteristics when designed with 1 mm



2020 JINST 15 P02021

**Table 1**. The dimension of the proposed UWB antenna.

| Parameter | Value (mm) | Parameter | Value (mm) |
|---|---|---|---|
| A | 20 | N | 30 |
| B | 2.07 | O | 1.37 |
| C, D | 10 | P | 4.75 |
| h | 3.7 | M | 42.5 |
| J | 15.8 | E | 2 |
| K | 20 | F | 3.14 |
| L | 8.3 | G | 17 |
| W | 2 | T | 4.14 |

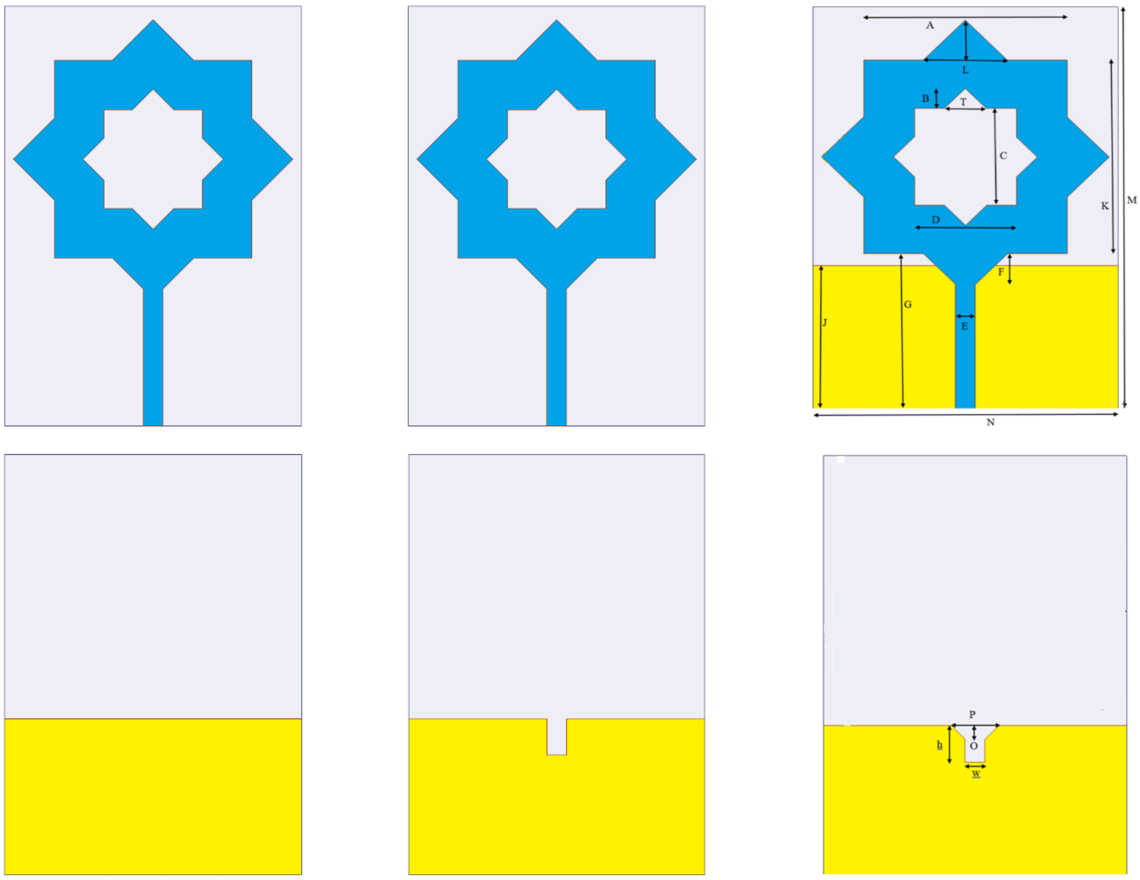


**(a)** **(b)** **(c)**

**Figure 1**. Design steps of proposed UWB antenna (a) Antenna-A, (b) Antenna-B, (c) proposed antenna.

wide ground slot. The antenna with 2 mm wide ground slot provides wide bandwidth ranging from 3.1 to 12.7 GHz and supports the bandwidth requirements for UWB systems. The −10 dB reflection co-efficient performance degrades with further increase in slot width. The 3 mm slot provides poor impedance matching at 6.15–7.85 GHz. The variations of the slot height "h" on the ground plane have a deep impact on the antenna performance. The antenna provides −10 dB bandwidth of 7 GHz

2020 JINST 15 P02021

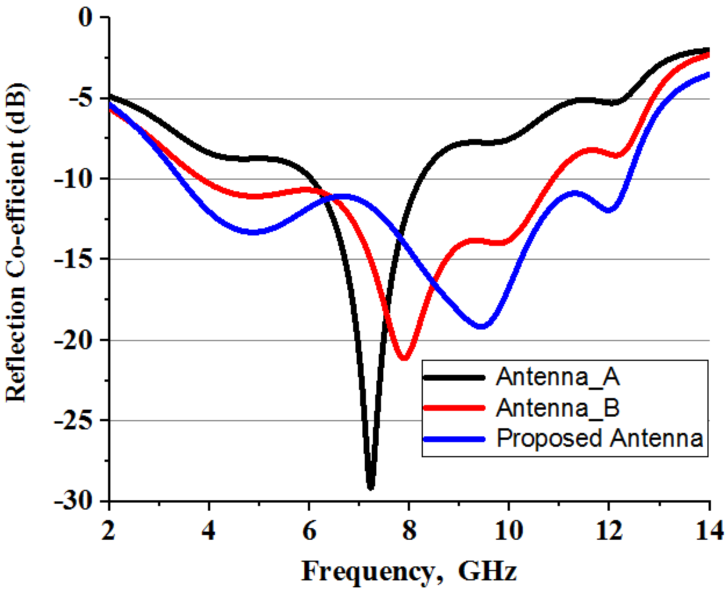


**Figure 2**. Simulated reflection coefficient of Antenna-A, B and proposed antenna.

(3.65–10.65 GHz) when the height of the slot is 1.7 mm. The antenna provides wider impedance bandwidth from 3.1 to 12.7 GHz for the slot height of 3.7 mm. When the slot height is further increased to 5.7 mm, the antenna provides poor return loss performance for a particular frequency band ranging from 5.75 to 7.3 GHz, which indicates undesired impedance matching and also the overall bandwidth of the antenna is reduced by 1100 MHz.

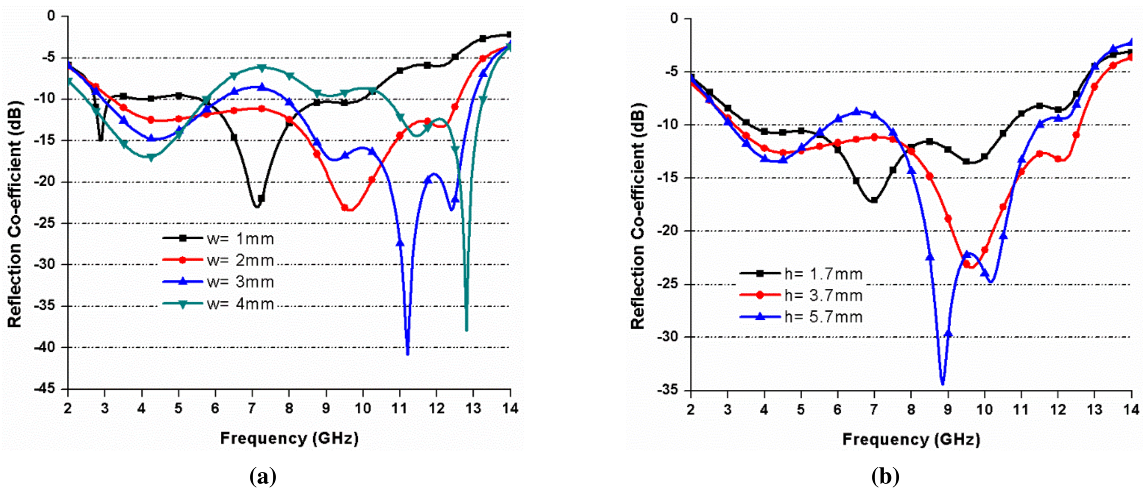


**Figure 3**. Antenna performance with the variations of (a) slot width, (b) slot height.

### 2.3 Radiation performance analysis

The surface current distribution, radiation pattern and gain parameter define the radiation performance of the antenna. The surface current distributions for the two pass band frequencies 4.76 GHz and 10 GHz are shown in figure 4. The current field is mainly concentrated on the outer edge of the lower part of the patch at the lower pass band frequency (4.76 GHz), whereas a relatively higher concentration of surface current distribution is observed at all the outer edge of the antenna patch for the upper band (10 GHz). The radiation patterns in terms of E-plane and H-Plane are shown in figure 5. It can be noticed that the E plane radiation pattern resembles like bi-directional at 4.76 GHz but the H plane pattern is purely omnidirectional in its shape. The radiation pattern of the antenna for the upper band frequency is slightly different and this may be due to the change in surface current distributions for 10 GHz. The E-plane and H-plane radiation pattern for the higher pass band frequency (10 GHz) shows highly concentrated radiation all over 360° except at some specific angles. The gain performance of the proposed UWB antenna is shown in figure 6. The high positive gain performance is observed all over the working frequency band. The peak gain of about 6 dBi is observed at 11.8 GHz. This positive gain and widespread radiation pattern ensure the stable performance of the antenna for the UWB applications.

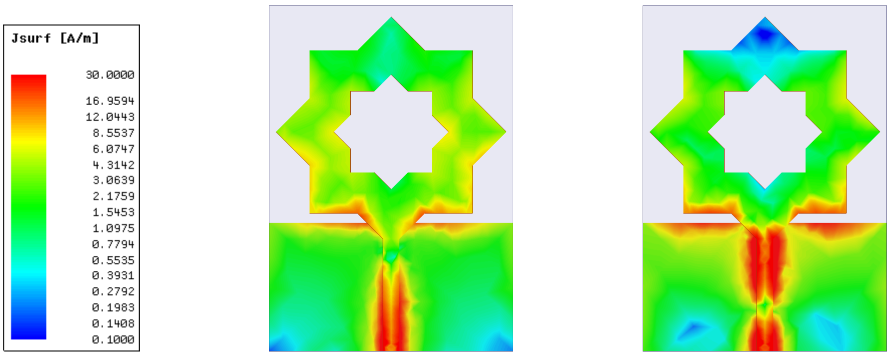


(a) (b)

**Figure 4**. Surface current distribution at two pass bands at (a) 4.76 GHz, (b) 10 GHz.

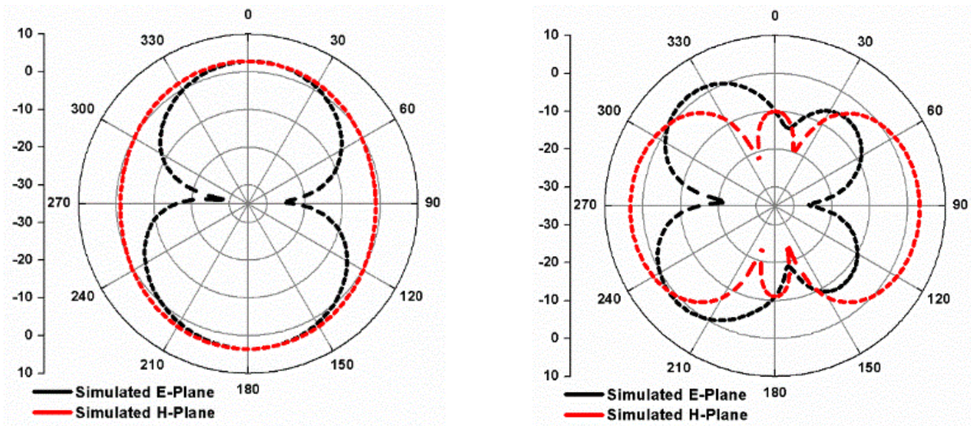


(a) (b)

**Figure 5**. E-plane and H-plane radiation pattern at (a) 4.76 GHz, (b) 10 GHz.



2020 JINST 15 P02021

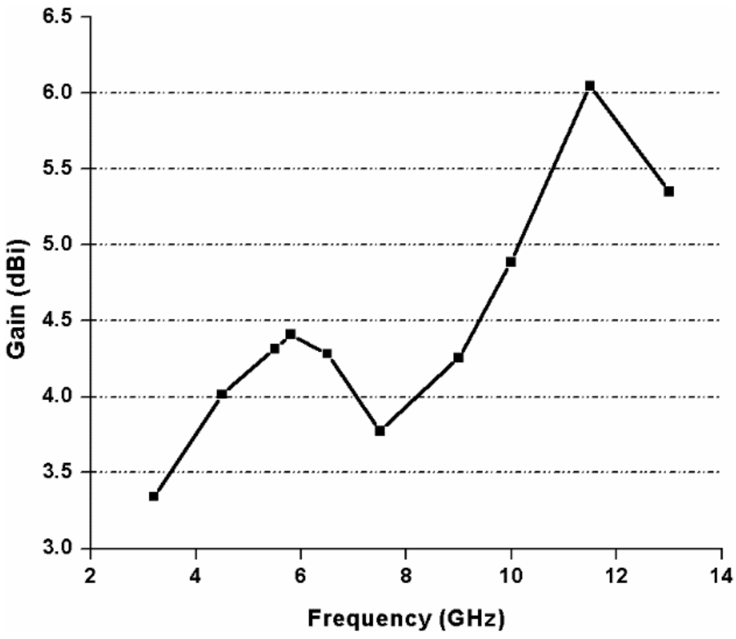


**Figure 6**. Gain performance.

### 2.4 Bending analysis

The flexible antenna should be enough robust and durable that can withstand in any situation without any major deviation in its performance. Figure 7a illustrates the bending deformation analysis of the proposed UWB antenna with various bending radius including 30 mm, 40 mm and 50 mm radius. The bending performance analysis of the antenna confirms its applicability in the flexible situation without any major deviation in reflection coefficient for different bending radius as shown in figure 7b. It can be noticed that the overall bandwidth of the antenna almost remains unaltered for different bending conditions.

## 3 Design of stop band filter for notched band functionality

The design of the stop band filter is very much essential for implementing the band rejection function on the proposed UWB antenna. An SRR (Split ring resonator) type stop band filter as shown in figure 8a is proposed for achieving wideband rejection function. The simulative responses of the split ring resonator stop band filter in terms of reflection coefficient ($S_{11}$) and transmission coefficient ($S_{21}$) are shown in figure 8b. This S-parameter curve confirms band rejection function of the stop band filter. This stop band filter is integrated with the developed UWB antenna to provide band rejection capability for wireless local area network (WLAN) IEEE802.11n (5.725–5.825 GHz) band.

## 4 Design of flexible UWB antenna with notched band characteristics

The analysis of the notched band characteristics of the UWB antenna on a flexible substrate is presented in this section. The structural geometry of the proposed band notched UWB antenna is

2020 JINST 15 P02021

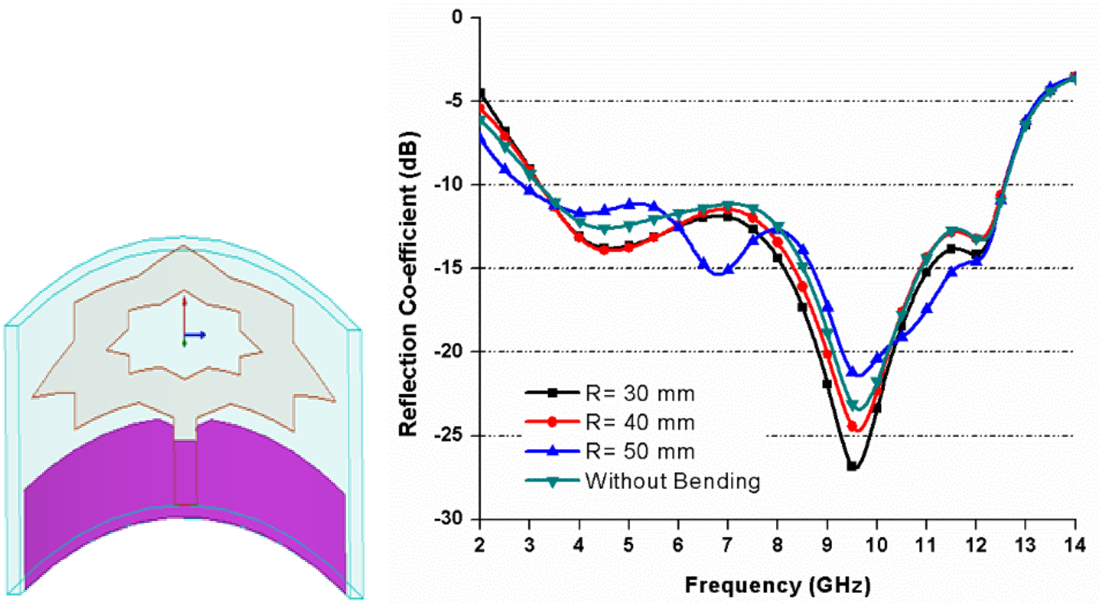


**(a)** **(b)**

**Figure 7**. Bending analysis (a) bending structure, (b) reflection coefficient with different radius.

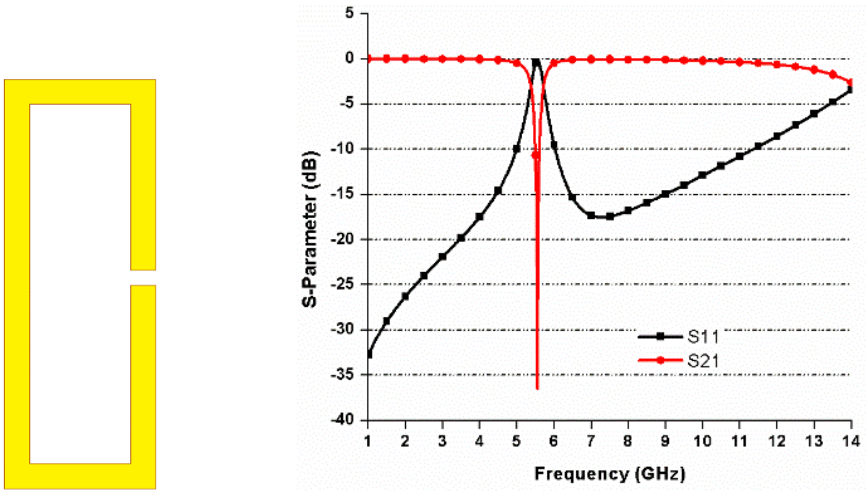


**(a)** **(b)**

**Figure 8**. (a) Structure of split ring resonator band stop filter, (b) S-parameter analysis.

shown in figure 9. The notched band characteristics are achieved by inserting the earlier discussed stop band filter on the ground plane of the UWB structure. This stop band filter interferes with the normal resonance response of the slot loaded octagonal star-shaped antenna and creates the notched band functionality. The gap parameter (S1) of the split ring resonator is responsible for controlling notch at the WLAN band as stated in table 2. The notched band response is shifted towards the higher frequency with the increase in gap dimension. Apart from that, the response of the UWB antenna shows that the bandwidth of the notched band also increases with the increase in the gap

2020 JINST 15 P02021

of the stop band filter as shown in figure 10. On the basis of the analysis of the stop band filter, the proposed antenna has been fabricated with a 0.3 mm gap in the SRR as it rejects major application frequency bands WLAN 5.8 GHz within its rejection bandwidth. The surface current distribution of the proposed UWB antenna validates the idea of rejection frequency bands. Figure 11 shows a high amount of surface current concentrated on the SRR for rejection band 5.8 GHz and relatively less amount of surface current is observed for the pass band frequencies at the lower band (4.76 GHz) and upper band (10 GHz).

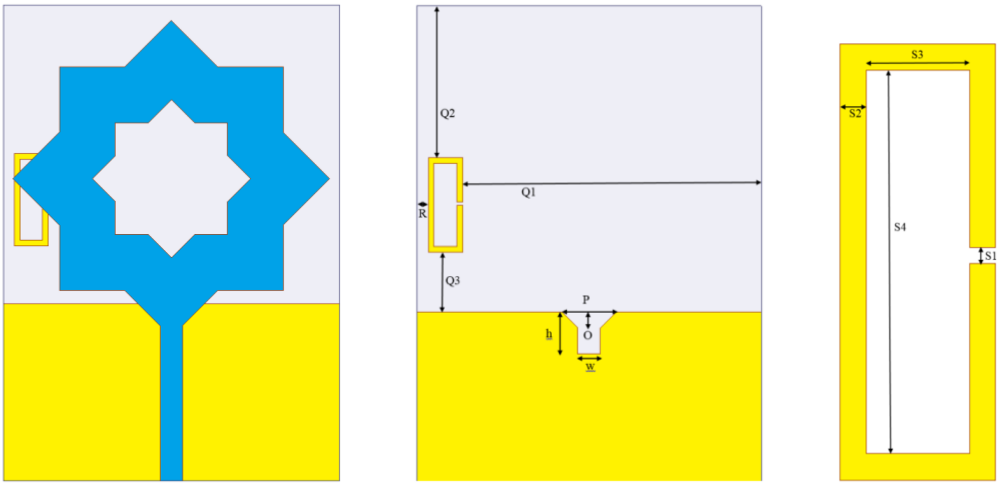


**Figure 9**. Structure of UWB antenna with rejection band, given parameters are Q1=26 mm, Q2=13.25 mm, Q3=5.2 mm, R, S3=2 mm, S1=0.3 mm, S2=0.5 mm, S4=7.25 mm.

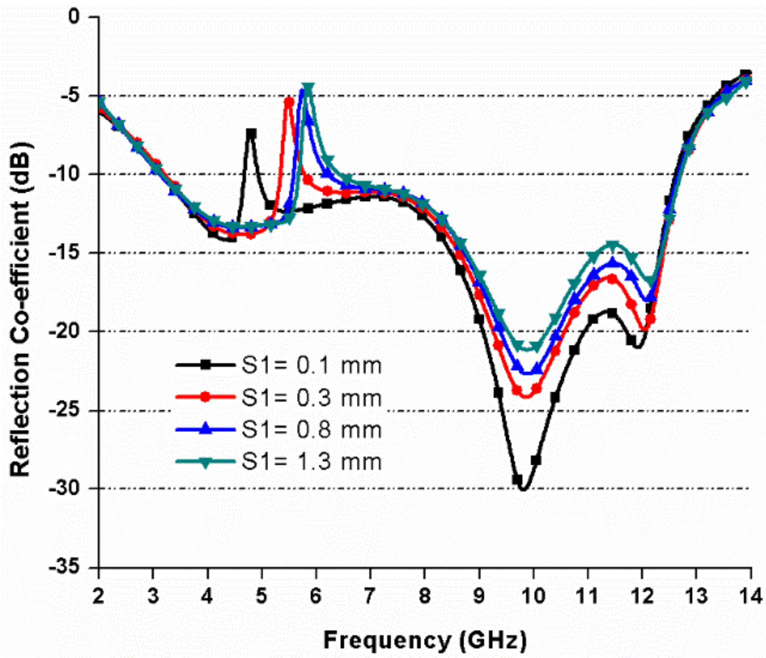


**Figure 10**. The variations of the notch band for different gaps of the band stop filter.

**Table 2**. Variation of notch band with SRR gap (S1).

| Gap (S1) | Notch frequency | Notch bandwidth |
|---|---|---|
| 0.1 mm | 4.7–4.9 GHz | 200 MHz |
| 0.3 mm | 5.6–6.0 GHz | 400 MHz |
| 0.8 mm | 5.8–6.3 GHz | 500 MHz |
| 1.3 mm | 5.85–6.4 GHz | 550 MHz |

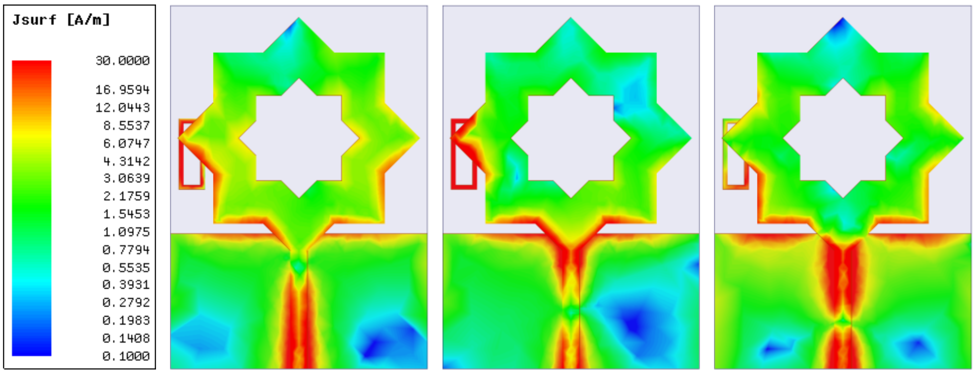


**(a)** **(b)** **(c)**

**Figure 11**. Surface current distribution at (a) pass band 4.76 GHz, (b) rejection band 5.8 GHz, (c) pass band 10 GHz.

## 5 Results and discussion

The prototype of the proposed octagonal UWB monopole antenna with notched band characteristics has been fabricated with optimal dimensions for validating the conceptual analysis. The prototype of the fabricated proposed antenna is shown in figure 12. The reflection coefficient of the proposed antenna has been measured using Anritsu MS2037C vector network analyzer. All radiation performances in terms of radiation patterns and gains are measured in an anechoic chamber. The comparison between the measured and simulation reflection coefficient of the proposed antenna is shown in figure 13. The measured performance depicts good agreement with the simulated results. The small deviation between simulated and measured results is mainly due to the tolerance in the fabrication process, connector loss, and environmental effect. However, the measured reflection coefficients confirm that the designed antenna can easily cover the bandwidth requirements for UWB systems. According to the measured result, as shown in figure 13b, a very low gain performance (–1.3 dBi) is observed over the rejection frequency bandwidth of 5.7 to 6.2 GHz. This notched band can avoid interference from IEEE802.11n specified standard for WLAN system. The simulated and measured gains of the proposed antenna in conformal conditions (Horizontal and Vertical) are depicted in figure 13c. It is observed that the antenna gain drops to a lower value (−2.45 dBi) at the notched band when the antenna is deformed with a bending radius 30 mm. It has been observed that the maximum gain of the antenna in the bending case for measurement result is 6.5 dBi at 11.8 GHz and the non-bending case is 6.7 dBi at 12.2 GHz. There is just a marginal difference of only 0.2 dBi. The simulated and measured radiation pattern of the proposed antenna in terms of E-plane and



2020 JINST 15 P02021

H-plane is shown in figure 14. It can be observed that the E-plane radiation pattern is bidirectional like dipole type whereas the H plane pattern for the same resembles purely omni-directional. The antenna shows widespread radiation for both E-plane and H-plane that indicates high gain at that particular frequency. The simulated and measured results of the proposed SRR based UWB antenna with notched band is arranged in table 3.

**Table 3**. Summarized results of the proposed band notched UWB antenna.

| Result | Lower Cut off Frequency | Upper Cut off Frequency | Fractional Bandwidth | Rejection Bandwidth | Peak Gain |
|---|---|---|---|---|---|
| Simulated | 3.1 GHz | 12.7 GHz | 121.5% (3.1–12.7 GHz) | 400 MHz (5.6–6 GHz) | 6.68 dBi |
| Measured | 3.25 GHz | 13 GHz | 120% (3.25–13 GHz) | 500 MHz (5.7–6.2 GHz) | 6.70 dBi |

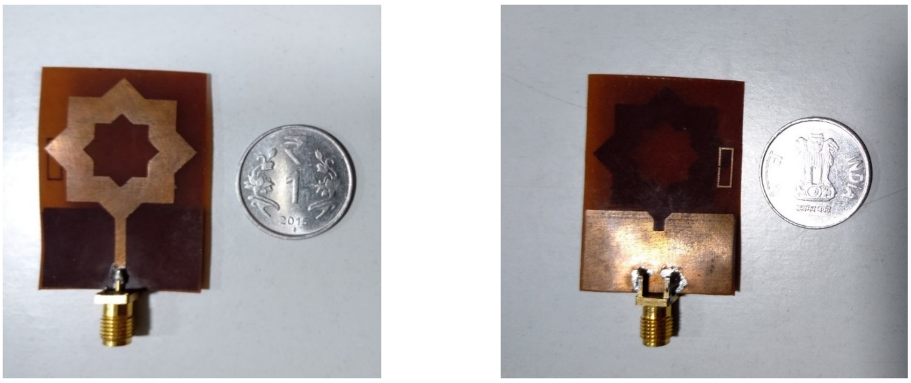

**Figure 12**. Fabricated prototype of proposed antenna.

The flexible antennas are a good candidate for a plane surface as well as for curved surface. The bending view of the fabricated prototype of the suggested antenna according to the surface is shown in figure 15a. The proposed antenna shows high robustness in the performance without any major deviation in its impedance bandwidth as depicted in figure 15b. Slight discrepancies between simulated and measured values are mainly due to bending losses. The surface current distribution of the proposed conformal antenna with bending radius R = 30 mm is depicted in figure 16. It has been observed that a high amount of surface current is mainly concentrated on the SRR for notched band 5.8 GHz which confirms the presence of notched band in bending conditions. The performance analysis of the antenna also shows that there is no major deviation in rejection frequency band for different bending radius. The performance comparisons of some recent flexible UWB antenna with our proposed design are shown in table 4. The proposed flexible antenna covers UWB bandwidth with a rejection frequency band for WLAN and good gain throughout the operating band.

The measurement setup is shown in figure 17 with the transmitting antenna of standard gain horn on the left side and the proposed antenna as receiving antenna on the right side. The radiation pattern and the gain is measured with turn table mechanism in the antenna measurement setup and driving software. Figure 18 shows the efficiency result of the proposed antenna in non bending, horizontal and vertical bending (R=30 mm) cases. The efficiency of the antenna drops at the notched band. It has been observed that the proposed flexible antenna is showing excellent performance

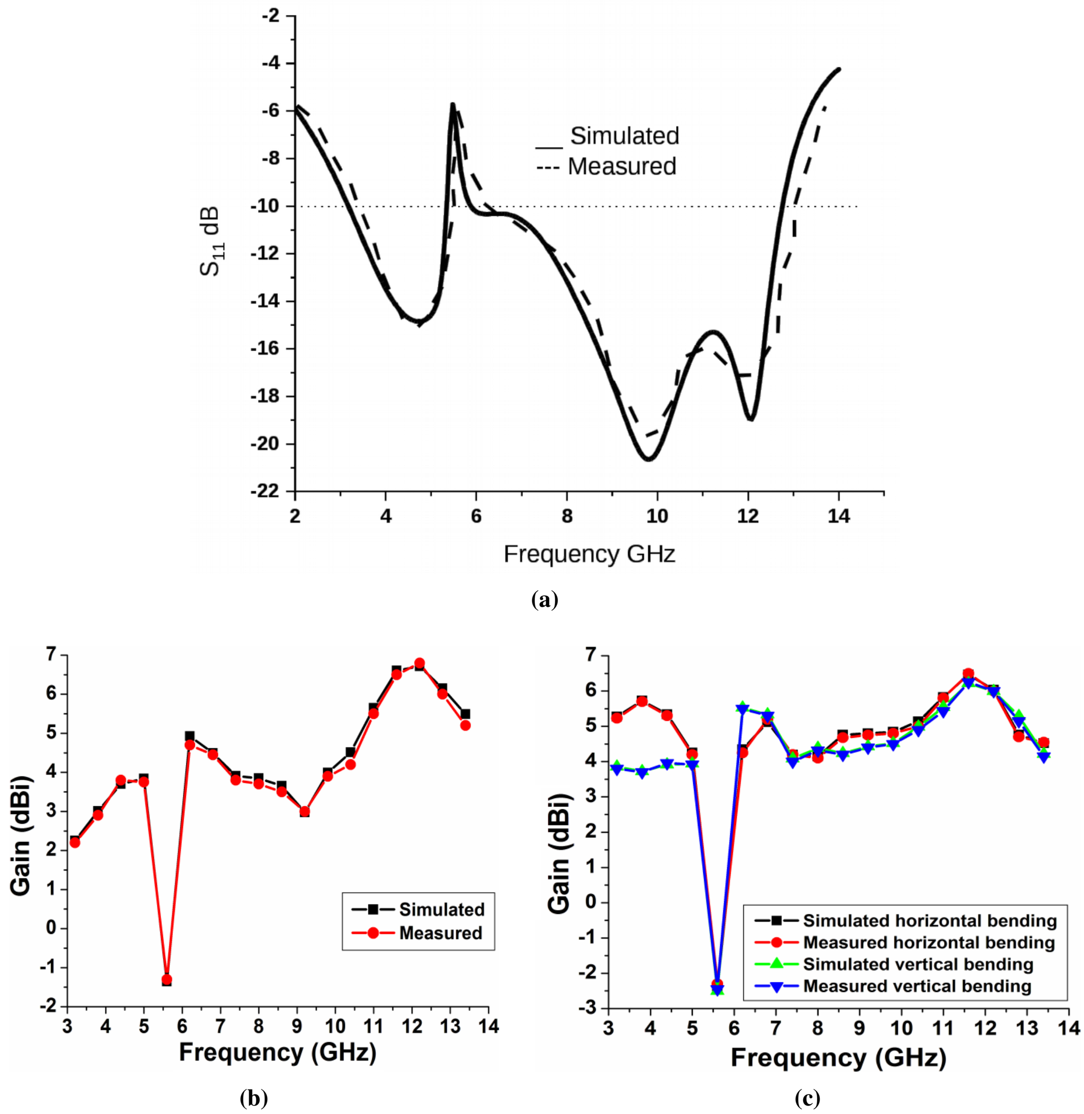


**Figure 13**. Simulated and Measured results (a) reflection coefficient, (b) gain without bending, (c) gain for horizontal and vertical bending with bending radius R = 30 mm.

**Table 4**. Performance comparisons of some recent flexible UWB antenna with the proposed Antenna.

| Ref. No. | Conformal | Dimension ($mm^2$) | Fractional Bandwidth | Rejection Bandwidth | Peak Gain |
|---|---|---|---|---|---|
| **9** | Yes | 6192 | 101% (10.6–3.5 GHz) | Not Available | 4.89 dBi |
| **10** | Yes | 1675.2 | 155% (8–1 GHz) | Not Available | 3.1 dBi |
| **11** | Yes | 880 | 125% (11–2.5 GHz) | Not available | 4.2 dBi |
| **13** | Yes | 722 | 119% (11.96–3.1 GHz) | Not Available | — |
| **16** | Yes | 1620 | 113% (12–3.3 GHz) | Not Available | 4.4 dBi |
| **17** | Yes | 1200 | 120% (12–3 GHz) | Not Available | 4 dBi |
| **18** | Yes | 8536 | 100% (10.3–3.4 GHz) | Not Available | 7.75 dBi |
| **19** | Yes | 416 | 110% (10.6–3.1 GHz) | 5.15–5.35 GHz | 3 dBi |
| **Proposed** | Yes | 1275 | 120% (13–3.25 GHz) | 5.7–6.2 GHz | 6.7 dBi |

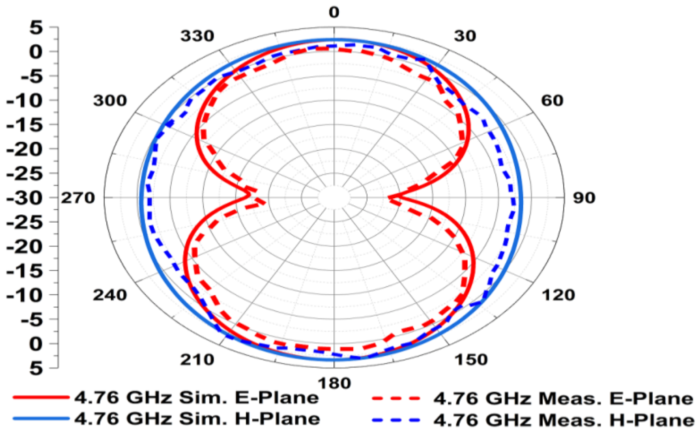


(a)

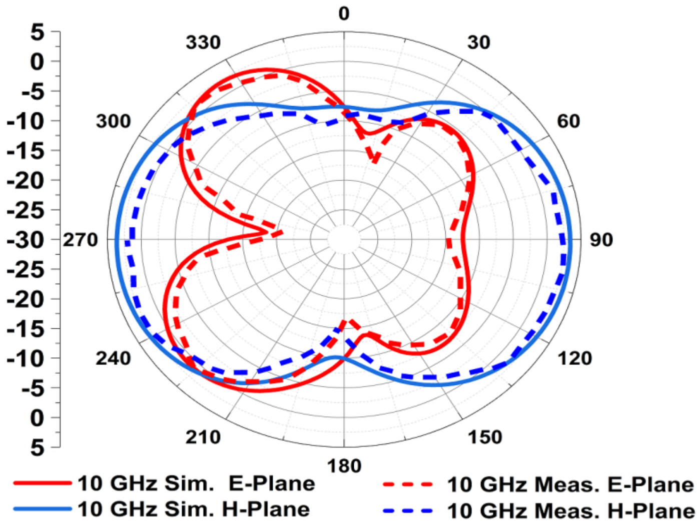


(b)

**Figure 14**. Simulated and measured radiation patterns (a) 4.76 GHz, (b) 10 GHz.

(a)

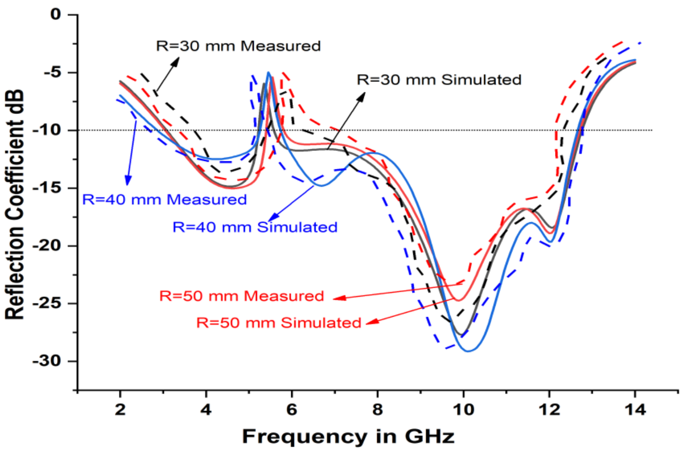


(b)

**Figure 15**. Flexibility analysis (a) view of bending setup of the fabricated prototype, (b) S-parameter.

2020 JINST 15 P02021

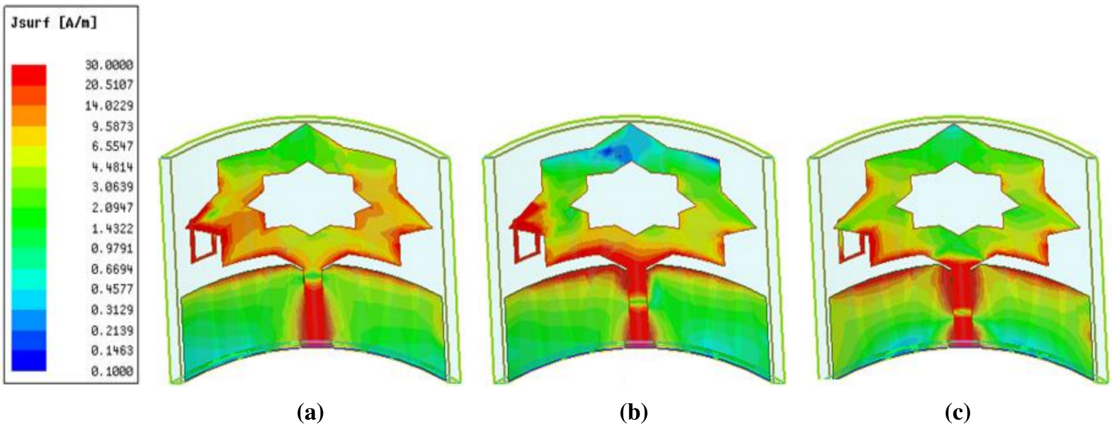


**Figure 16**. Surface current distribution of the proposed conformal antenna with bending radius R = 30 mm at (a) pass band 4.76 GHz, (b) rejection band 5.8 GHz, (c) pass band 10 GHz.

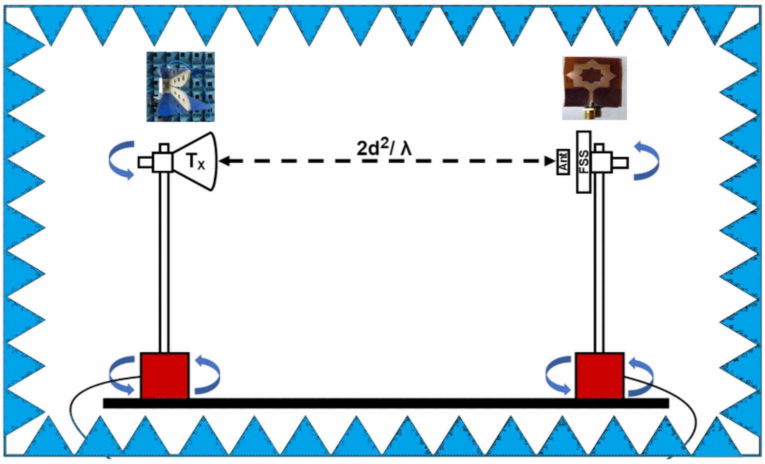


**Figure 17**. Antenna measurement setup.

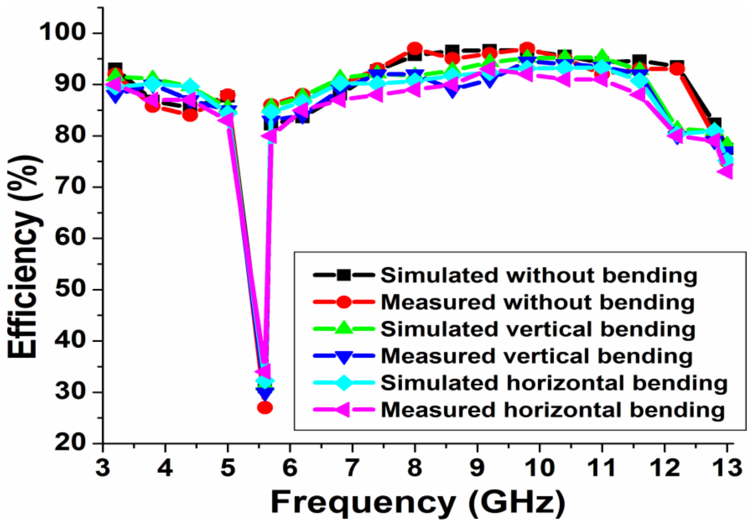


**Figure 18**. Efficiency vs. Frequency in non bending and bending (horiontal and vertical conditions).

characteristics with almost no change in the efficiency at bending also. This shows the consistency of the antenna in conformal conditions and applicability at different host surfaces.

**Conclusion.** A flexible ultra-wideband antenna with a rejection band for high speed WLAN applications is presented in this paper. This flexible monopole antenna is fabricated on a thin and compact conformable Teflon substrate. A partial ground plane octagonal star slot loaded patch fed by a microstrip line has been embedded to achieve wide impedance bandwidth over the UWB band ranging from 3.25 GHz to 13 GHz with a peak gain of 6.7 dBi. The proposed antenna has been fabricated with a 0.3 mm SRR gap for eliminating IEEE802.11n (5.725–5.825 GHz) WLAN band. In addition, the antenna provides minor deviation in terms of impedance bandwidth and rejection band for different bending situations. This high robustness in bending, stable widespread radiation pattern with high gain makes the antenna a suitable choice for UWB communication systems.


## Acknowledgments

The authors would like to thank DST for the technical support through ECR/2016/000569 and EEQ/2106/000604 and also the ALRC-R&D of KL University, A.P., INDIA for fabrication and the measurement support.


## References


[1] P. Gentner, G. Hilton, M. Beach and C. Mecklenbräuker, *Characterisation of ultra-wideband antenna arrays with spacings following a geometric progression*, *IET Commun.* **6** (2012) 1179.

[2] ECC, *CEPT Report 45. Report from CEPT to the European Commission in response to the Fifth Mandate to CEPT on ultra-wideband technology to clarify the technical parameters in view of a potential update of Commission Decision 2007/131/EC*, ECC (2013) and online pdf version at https://www.ecodocdb.dk/download/8bc53456-a8a0/CEPTREP045.PDF.

[3] A. Sharma, G. Das and R.K. Gangwar, *Composite antenna for ultrawide bandwidth applications: Exploring conceptual design strategies and analysis*, *IEEE Antennas Propag. Mag.* **60** (2018) 57.

[4] S. Guruswamy, R. Chinniah and K. Thangavelu, *A printed compact UWB Vivaldi antenna with hemi cylindrical slots and directors for microwave imaging applications*, *Int. J. Electron. Commun.* **110** (2019) 152870.

[5] B. Biswas, R. Ghatak and D.R. Poddar, *UWB monopole antenna with multiple fractal slots for band-notch characteristic and integrated bluetooth functionality*, *J. Electromagn. Waves Appl.* **29** (2015) 1593.

[6] M.A. Salamin, W.A. Ali, S. Das and A. Zugari, *Design and investigation of a multi-functional antenna with variable wideband/notched UWB behavior for WLAN/X-band/UWB and Ku-band applications*, *Int. J. Electron. Commun.* **111** (2019) 152895.

[7] G. Mishra and S. Sahu, *Compact circular patch UWB antenna with WLAN band notch characteristics*, *Microwave Opt. Technol. Lett.* **58** (2016) 1068.

[8] M. Salamin, W. Ali and A. Zugari, *A novel UWB antenna using capacitively-loaded fork-shaped resonator and modified fork-shaped DMS for interference mitigation with WiMAX and WLAN applications*, 2019 *JINST* **14** P03008.

[9] K. Shafique, B.A. Khawaja, M.A. Tarar, B.M. Khan, M. Mustaqim and A. Raza, *A wearable ultra-wideband antenna for wireless body area networks*, *Microwave Opt. Technol. Lett.* **58** (2016) 1710.

[10] Z. Hamouda, J.-L. Wojkiewicz, A.A. Pud, L. Kone, S. Bergheul and T. Lasri, *Flexible UWB organic antenna for wearable technologies application*, *IET Microw. Antennas Propag.* **12** (2018) 160.

[11] S.R. Zahran, M.A. Abdalla and A. Gaafar, *Time domain analysis for foldable thin UWB monopole antenna*, *Int. J. Electron. Commun.* **83** (2018) 253.

[12] J.R. Flores-Cuadras, J.L. Medina-Monroy, R.A. Chavez-Perez and H. Lobato-Morales, *Novel ultra-wideband flexible antenna for wearable wrist worn devices with 4G LTE communications*, *Microwave Opt. Technol. Lett.* **59** (2017) 777.

[13] L.-J. Xu, H. Wang, Y. Chang and Y. Bo, *A flexible UWB inverted-F antenna for wearable application*, *Microwave Opt. Technol. Lett.* **59** (2017) 2514 [*Erratum ibid.* **60** (2018) 281].

[14] T.K. Saha, T.N. Knaus, A. Khosla and P.K. Sekhar, *A CPW-fed flexible UWB antenna for IoT applications*, *Microsyst. Technol. 15 December 2018*.

[15] H.A.E. Elobaid, S.K.A. Rahim, M. Himdi, X. Castel and M.A. Kasgari, *A transparent and flexible polymer-fabric tissue UWB antenna for future wireless networks*, *IEEE Antennas Wirel. Propag. Lett.* **16** (2017) 1333.

[16] H.A. Elmobarak, S.K.A. Rahim, X. Castel and M. Himdi, *Flexible conductive fabric/E-glass fibre composite ultra-wideband antenna for future wireless networks*, *IET Microw. Antennas Propag.* **13** (2019) 455.

[17] Y. Sun, T.I. Yuk and S.W. Cheung, *Design of a textile ultra-wideband antenna with stable performance for body-centric wireless communications*, *IET Microw. Antennas Propag.* **8** (2014) 1363.

[18] P.B. Samal, P.J. Soh and G.A.E. Vandenbosch, *UWB all-textile antenna with full ground plane for off-body WBAN communications*, *IEEE Trans. Antennas Propag.* **62** (2014) 102.

[19] Q.H. Abbasi, M.U. Rehman, X. Yang, A. Alomainy, K. Qaraqe and E. Serpedin, *Ultrawideband band-notched flexible antenna for wearable applications*, *IEEE Antennas Wirel. Propag. Lett.* **12** (2013) 1606.